Can J Anesth/J Can Anesth (2011) 58:191–205
DOI 10.1007/s12630-010-9419-9

THEME ISSUE: MECHANISMS OF ANESTHESIA

Anesthetic sites and allosteric mechanisms of action on Cys-loop ligand-gated ion channels

Les sites anesthésiques et les mécanismes d'action allostériques sur les canaux ioniques sensibles à un ligand sur la boucle Cys

Stuart A. Forman, MD · Keith W. Miller, DPhil

Received: 17 September 2010 / Accepted: 26 October 2010 / Published online: 7 January 2011

Abstract

Purpose *The Cys-loop ligand-gated ion channel superfamily is a major group of neurotransmitter-activated receptors in the central and peripheral nervous system. The superfamily includes inhibitory receptors stimulated by γ-aminobutyric acid (GABA) and glycine and excitatory receptors stimulated by acetylcholine and serotonin. The first part of this review presents current evidence on the location of the anesthetic binding sites on these channels and the mechanism by which binding to these sites alters their function. The second part of the review addresses the basis for this selectivity, and the third part describes the predictive power of a quantitative allosteric model showing the actions of etomidate on γ-aminobutyric acid type A receptors ($GABA_ARs$).*

Principal findings *General anesthetics at clinical concentrations inhibit the excitatory receptors and enhance the inhibitory receptors. The location of general anesthetic binding sites on these receptors is being defined by photoactivable analogues of general anesthetics. The receptor studied most extensively is the muscle-type nicotinic acetylcholine receptor (nAChR), and progress is now being made with $GABA_ARs$. There are three categories of sites that are all in the transmembrane domain: 1) within a single subunit's four-helix bundle (intrasubunit site; halothane and etomidate on the δ subunit of AChRs); 2) between five subunits in the transmembrane conduction pore (channel lumen sites; etomidate and alcohols on nAChR); and 3) between two subunits (subunit interface sites; etomidate between the α1 and β2/3 subunits of the $GABA_AR$).*

Conclusions *These binding sites function allosterically. Certain conformations of a receptor bind the anesthetic with greater affinity than others. Time-resolved photolabelling of some sites occurs within milliseconds of channel opening on the nAChR but not before. In $GABA_ARs$, electrophysiological data fit an allosteric model in which etomidate binds to and stabilizes the open state, increasing both the fraction of open channels and their lifetime. As predicted by the model, the channel-stabilizing action of etomidate is so strong that higher concentrations open the channel in the absence of agonist. The formal functional paradigm presented for etomidate may apply to other potent general anesthetic drugs. Combining photolabelling with structure-function mutational studies in the context of allosteric mechanisms should lead us to a more detailed understanding of how and where these important drugs act.*

Résumé

Objectif *La superfamille des canaux ioniques sensibles à un ligand sur la boucle Cys constitue un important groupe de récepteurs activés par les neurotransmetteurs dans les systèmes nerveux central et périphérique. Cette superfamille comprend des récepteurs inhibiteurs stimulés par l'acide γ-aminobutyrique (GABA) et la glycine ainsi que des récepteurs excitateurs stimulés par l'acétylcholine et la sérotonine. La première partie de ce compte-rendu présente les données probantes actuelles sur l'emplacement*

This article is accompanied by an editorial. Please see Can J Anesth 2011; 58(2).

S. A. Forman, MD (✉) · K. W. Miller, DPhil
Department of Anesthesia, Critical Care & Pain Medicine, Massachusetts General Hospital, Jackson 444, Boston, MA 02114, USA
e-mail: saforman@partners.org

K. W. Miller, DPhil
Department of Biological Chemistry and Molecular Pharmacology, Harvard Medical School, Boston, MA, USA

des sites de liaison des anesthésiques sur ces canaux et le mécanisme par lequel la liaison sur ces sites en particulier modifie leur fonctionnement. La deuxième partie de notre article traite des bases de cette sélectivité, et la troisième partie décrit le pouvoir de prédiction d'un modèle allostérique quantitatif montrant l'effet de l'étomidate sur les récepteurs d'acide γ-aminobutyrique de type A (R-GABA$_A$).

Constatations principales *Les anesthésiques généraux administrés en concentrations cliniques inhibent les récepteurs excitateurs et stimulent les récepteurs inhibiteurs. L'emplacement des sites de liaison des anesthésiques généraux sur ces récepteurs est défini par des analogues photoactivés des anesthésiques généraux. Le récepteur qui a été le mieux étudié est le récepteur nicotinique de l'acétylcholine (RnACh) de type musculaire, et des progrès voient actuellement le jour dans nos connaissances des R-GABA$_A$. Il existe trois catégories de sites, tous situés dans le domaine transmembranaire : 1) à l'intérieur du faisceau à quatre hélices d'une seule sous-unité (site intra-sous-unité; l'halothane et l'étomidate sur la sous-unité δ des RACh); 2) entre cinq sous-unités dans le pore de conduction transmembranaire (sites dans la lumière des canaux; l'étomidate et les alcools sur le RnACh); et 3) entre deux sous-unités (sites d'interface de sous-unités; l'étomidate entre les sous-unités α1 et β2/3 du R-GABA$_A$).*

Conclusion *Ces sites de liaison fonctionnent de façon allostérique. Certaines conformations d'un récepteur lient l'anesthésique avec une plus grande affinité que d'autres. Le marquage par photoaffinité en temps différé de certains sites survient dans les millisecondes suivant l'ouverture du canal sur le RnACh, mais pas avant. Dans les R-GABA$_A$, les données électrophysiologiques sont conformes à un modèle allostérique dans lequel l'étomidate se lie et stabilise l'état ouvert, ce qui augmente la fraction des canaux ouverts et leur durée de vie. Comme notre modèle l'a prédit, l'action de stabilisation des canaux de l'étomidate est tellement puissante que des concentrations élevées ouvrent les canaux en l'absence d'un agoniste. Le paradigme de fonctionnement formel présenté pour l'étomidate pourrait s'appliquer à d'autres agents anesthésiques généraux puissants. La combinaison du marquage par photoaffinité et d'études de mutation de fonction de structure dans le contexte des mécanismes allostériques devrait nous permettre de mieux comprendre où et comment ces importants médicaments agissent.*

Research on the molecular mechanisms of general anesthesia continues to focus on Cys-loop ligand-gated ion channels, as evidence continues to accumulate implicating the gamma-aminobutyric acid-A ($GABA_A$) receptors in major anesthetic actions, the glycine receptor in immobility, and the nAChRs in memory, autonomic functions, and neuromuscular relaxation.[1-7] Furthermore, our understanding of how and where general anesthetics modulate these targets has progressed dramatically. This review presents current evidence on the location of the anesthetic binding sites on these channels and the mechanism by which binding to these sites alters their function. The best-characterized mechanisms involve selective allosteric interactions of general anesthetics with the open state of these channels; hence, the second part of the review addresses the basis for this selectivity. The third part describes the predictive power of a quantitative allosteric model of the actions of etomidate on $GABA_A$Rs.

Allosterism and binding sites

An elegant exposition on allosterism first appeared 45 years ago.[8-10] Today it is an accepted concept with ramifications that extend to medicine,[11] signal transduction,[12,13] and anesthetic action.[14-18] The affinity of an allosteric anesthetic binding site requires that the site should be higher in certain conformations than in others. In this way, the anesthetic stabilizes certain conformations over others. Thus, consider a protein that contains a single anesthetic binding site that can exist in three different native conformations each of which has a different affinity for anesthetics (Fig. 1). The fraction of the protein in a given conformation depends on its free energy. When an anesthetic binds to only one of the conformations, its free energy is decreased by the binding free energy so that the fraction of the protein in that conformation increases. If such a conformation were the open-channel state of a ligand-gated ion channel, the fraction of channels open would be increased and their lifetime likely would be longer and more current would pass. This is the case with $GABA_A$Rs.[15] A special case occurs if the stabilizing anesthetic binding site is situated in the channel lumen. In nAChRs, many agents cause open channel inhibition. The anesthetic has higher affinity for the open state and binds to it as soon as the agonist opens the channel, but once bound, it sterically obstructs the flow of ions through the channel.

Two main factors determine the affinity of an anesthetic for a binding pocket. First, the attractive energy falls off very rapidly with distance, so a snug fit is needed, which means that the pocket must be comparable in size with the anesthetic (conformation 2, Fig. 1). The maximum attraction occurs when two atoms are separated by only 12-20% (the distance increases with polarity) of the sum of their radii (for a review see[19]). Second, the pocket cannot be smaller than the anesthetic because the repulsive energy increases very rapidly as two atoms approach each other (they interact as hard spheres). Thus, an anesthetic can't

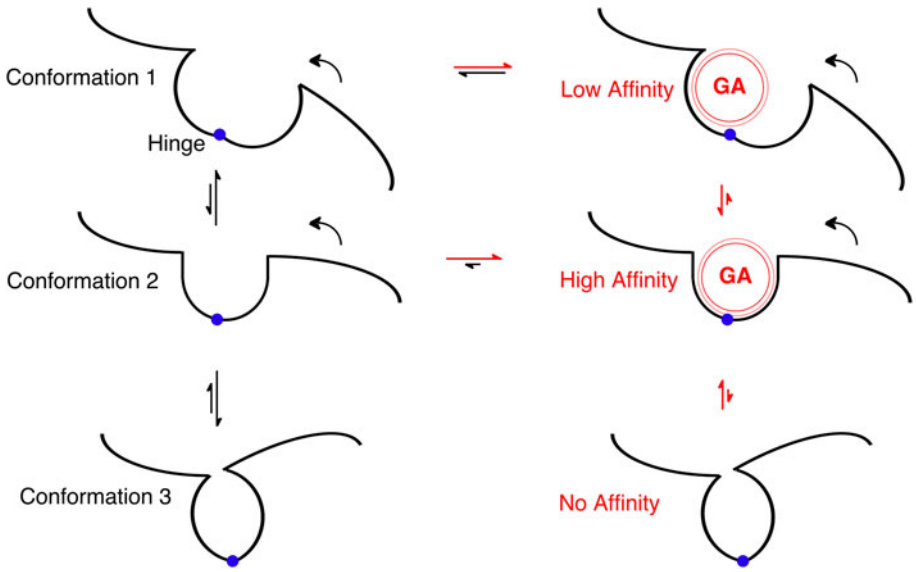

Fig. 1 Principles of allosterism. The black lines depict part of a protein in a region where two domains are joined by a structural hinge (blue circle). In the left-hand column, the protein can adopt three different conformations depending on movement of the right-hand domain around the hinge (curved arrows). The relative size of the two black vertical straight arrows between each pair of conformations suggests the equilibrium distribution between the conformations. Conformations 1 and 3 are favoured relative to Conformation 2. In the right-hand column, general anesthetics (GA; red sphere) have the opportunity to bind to each of these conformations in the pocket between the domains. Since the intermolecular dispersion forces between the general anesthetic and the protein are very short range (depicted by the thin red outer line), strong, high-affinity interactions occur only when the anesthetic fits snugly in the pocket (i.e., in Conformation 2). If the hinge closes too far (Conformation 3), steric hindrance prevents the anesthetic from binding. The horizontal red and black arrows depict how anesthetic binding perturbs the equilibrium between anesthetic free (left) and anesthetic bound (right) protein. In this example, Conformation 2 is sufficiently stabilized by the anesthetic's binding energy, which it is now the most stable relative to Conformations 1 and 3

squeeze down into a smaller pocket. Due to these constraints, a binding site that changes its geometry with the protein's conformation will bind the anesthetic tightly in only one conformation (Fig. 1).

The structure of Cys-loop ligand-gated ion channels

In order to resolve anesthetics bound to a protein in atomic detail, a resolution of 2 Å is required. In addition, to understand allosterism, the same structure should be determined in several conformations. However, currently there are no structures of mammalian Cys-loop ligand-gated ion channels that achieve this resolution. The only structure of a vertebrate receptor is the cryoelectron microscopy structure of the muscle subtype of the acetylcholine receptor from *Torpedo* electric tissue, which is determined in the absence of agonist in the resting or closed state at 4 Å resolution.[20] Such resolution is not sufficient to resolve the detailed structure of the amino acid side chains, let alone the presence of an anesthetic. The only other structures that include the transmembrane domain are those recently determined for two bacterial members of the same superfamily.[21,22] Although they lack the intracellular domain, they confirm the secondary structure of the transmembrane and extracellular domains seen in the cryoelectron microscopy structure above. One structure, ELIC, is thought to be in the closed state. The other protein, GLIC, is thought to be in the open state, but there is no independent confirmation of this, and no structure of a single receptor in more than one state has been determined. Nonetheless, the bacterial channels' structures are of sufficient resolution to allow bound anesthetics to be detected. Xenon has been imaged in the ELIC structure near the top of the pore. GLIC is sensitive to anesthetics,[23] and bound anesthetic can be detected crystallographically.[24]

The cryoelectron microscopy structure of the *Torpedo* nAChR is shown in Fig. 2A. Each of the five subunits consists of three domains. First, an extracellular domain of some 200 residues that binds the agonist and that largely consists of a β-sheet structure. Second, a transmembrane domain containing four α-helices arranged as a four-helix bundle (M1 – M4; Fig. 2B), in which M1 and M2 and M2 and M3 are separated by short loops. Third, there is a long intracellular loop between M3 and M4, much of whose structure could not be defined. The secondary structure of the bacterial channels is similar, although the lengths of the transmembrane helices and loops differ, and there is a short intercellular domain between M3 and M4. Thus, it seems reasonable to assume that other members of the

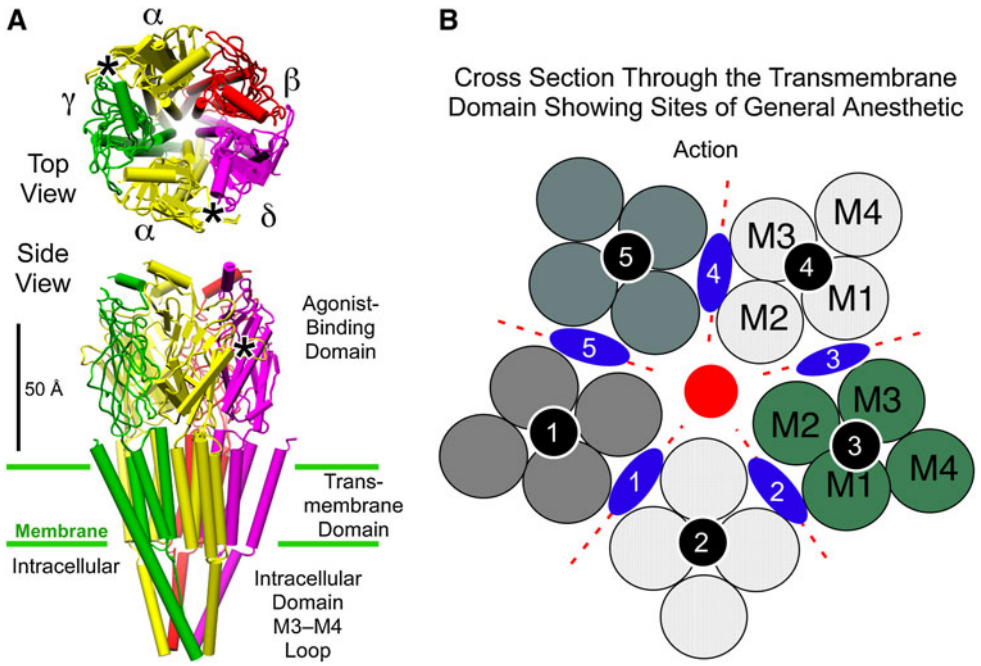

Fig. 2 General anesthetic binding sites on ligand-gated ion channels of the Cys-loop receptor superfamily. *Panel A* shows the structure of the nicotinic acetylcholine receptor (Unwin 2005) with its five subunits arranged centro-symmetrically around a central ion pore or channel, in both top view from the extracellular side and side view. The agonist site (*) in the extracellular agonist-binding domain is on the α-subunits in the interface with the γ- and δ-subunits. *Panel B* shows a schematic of a cross section through the transmembrane region. Each subunit, separated by dotted red lines, consists of four transmembrane helices shown as circles and numbered in the order they appear in the sequence. Three categories of anesthetic binding site (see text) are superimposed; intrasubunit sites (black circles); a channel lumen site (red circle), and subunit interface sites (blue lozenges). Molecular graphics images were produced using the University of California, San Francisco Chimera package from the Resource for Biocomputing, Visualization, and Informatics at the University of California, San Francisco (supported by NIH P41 RR-01081)[74]

superfamily, particularly the $GABA_A$Rs, have a similar secondary structure (see below). To facilitate the following discussion of photolabelling of the channel lumen, which is bounded by the M2 helices of five subunits, we use the prime numbering system for residues that aligns the M2 helix of all receptor subunits in such a way that the conserved leucine is always at M2–9′.

A high resolution structure of the $GABA_A$Rs is not yet available. In such situations, structural biologists build a homology model. This is achieved by using a known published structure from the same superfamily, aligning its sequence with the new receptor, and substituting the residues of the new receptor onto the known structure. Finally, energy minimization is performed to sort out steric clashes and optimize positive interactions, such as H-bonds or charge-charge interactions. In a sense, the homology model is just a three-dimensional alignment algorithm. It should be regarded as providing no more than a hypothesis or cartoon for designing experiments. Indeed, the homology models from different research groups often differ in detail.[25,26] Generally, the secondary structure is conserved within the superfamily, and the variation between models arises mainly from uncertainties in how to align the sequences, e.g., the length of the M2 – M3 loop differs in nAChR and $GABA_A$Rs, introducing considerable uncertainty in the alignment of M3.[27] Cross-linking of introduced cysteines can reduce the uncertainties to some extent.[28,29]

Within the framework of these structures, photolabelling has defined three categories of general anesthetic sites in the transmembrane domain of ligand-gated ion channels. We outline them here before considering the detailed results. First, there is an intrasubunit site (Fig. 2B, black circles) located within the four-helix bundle of individual subunits; halothane and etomidate can bind here on the nAChR. Second, there is a channel lumen site (Fig. 2B, red circle) located between all five subunits; alcohols and etomidate can bind here on the nAChR. Third, there is a subunit interface site (Fig. 2B, blue lozenges) located between the subunits in the subunit-subunit interfaces; etomidate binds here on the $GABA_A$R. Note the importance of the subunit composition. A homomeric receptor, such as the glycine or the serotonin type 3A receptor, might have five copies of one subunit interface site; whereas, a

receptor consisting of three different subunits, such as certain $GABA_A$Rs, has more possibilities.

The art of photolabelling

Currently, the only unambiguous information on the location of general anesthetic sites on different conformations of a given mammalian receptor comes from photolabelling studies. The method involves developing and characterizing new general anesthetics that have the additional property of becoming chemically reactive when exposed to light of a certain wavelength. If this process occurs while the agent is bound to its target ion channel, it becomes possible to identify residues in contact with the agent in its binding pocket. The main limitations of this approach follow from the fact that the amino acid sequencing required is very difficult because of the hydrophobicity of the transmembrane domain where the anesthetic sites are located. Large amounts of protein are required to overcome this hurdle, and the most detailed information is available for the *Torpedo* acetylcholine receptor because it is readily available in adequate quantity. However, recent progress in the heterologous expression of human neuronal $GABA_A$Rs largely resolves this problem.[30]

Here we review the location of general anesthetic sites established by photolabelling with halothane, two etomidate derivatives, and 3-azioctanol (Fig. 3). Each of these has advantages and disadvantages that we point out in the appropriate sections. Furthermore, to avoid discussing nonspecific binding, the emphasis is on sites where the degree of photoincorporation is modulated by changes in conformation between the equilibrium resting and the desensitized states of the receptor. How these sites change during gating is considered in a subsequent section.

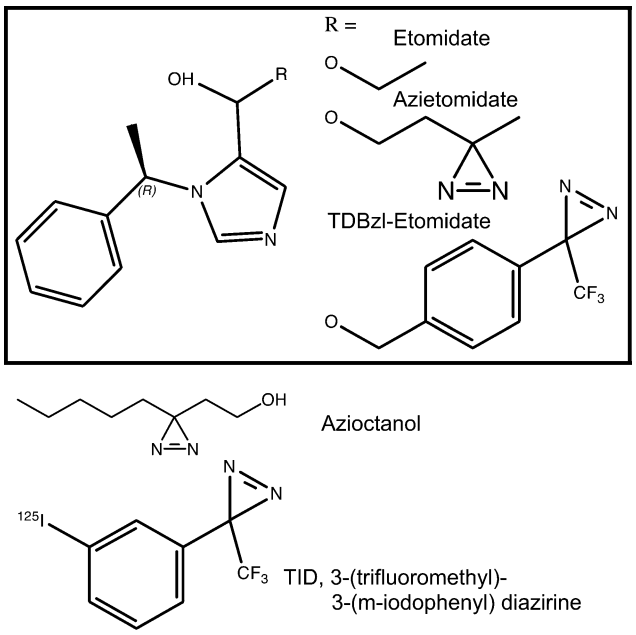

Fig. 3 Formulae of photolabels referred to herein

Location of general anesthetic sites on nicotinic acetylcholine receptors

Halothane was the earliest photoactivable anesthetic.[31,32] It reacts covalently with tyrosines and tryptophans and can tell us about binding pockets that contain these residues. Unfortunately, some regions of interest, e.g., the channel lumen, lack such residues. However, halothane does not react with all of the tyrosines and tryptophans in the nAChR; hence, those it does react with likely represent true binding sites. In the transmembrane domain, halothane photoincorporated into δY228 at higher levels in the desensitized state than in the resting state. It also photolabelled the equivalent residue on the α-subunits, αY213, but at a level too low to assess state-dependence (see Fig. 4A). These residues are at the extracellular end of M1, two helical turns above the conserved proline. On the nAChR structure, δY228 faces into an intrasubunit site within the four-helix bundle. In the α-subunit, there is one more residue between the tyrosine and the conserved proline, so that the two copies of αY213 face into the α-β and α-γ intersubunit interfaces, which may explain why they are labelled tenfold less than δY228.

Halothane's photochemistry is not ideal because it is activated by wavelengths of light that also activate bonds in the protein. Diazirines, like azioctanol,[33] azietomidate[34] and azi-isoflurane[35] (Fig. 3), do not have this disadvantage. In the transmembrane domain, 3-azioctanol, an open-state inhibitor of the ion channel,[33] photolabels the α-subunit at αE262 M2–20′. It is near the top of M2 and points into the channel lumen[36] (Fig. 4A and B). It is located above a largely hydrophobic region of the channel lumen that stretches down to the conserved αL251 (M2–9′), so it is tempting to assume that the hydrophobic tail of the alcohol projects in the intracellular direction down the channel. However, this hypothesis remains untestable because hydrophobic residues rarely react with aliphatic diazirines.

In anesthetics that have more complex chemical structures, it is possible to insert either an aliphatic or an aromatic diazirine at a particular position. Since each type of diazirine reacts with a different spectrum of residues, such a pair of general anesthetics would skirt the issue of each photolabel exhibiting certain "blind spots". Such a pair of derivatives has been added to the etomidate structure (Fig. 3) to provide a more complete picture of sites on the nAChR. The first of these was azietomidate, an aliphatic diazirine. Like 3-azioctanol, it photolabels αE262 on

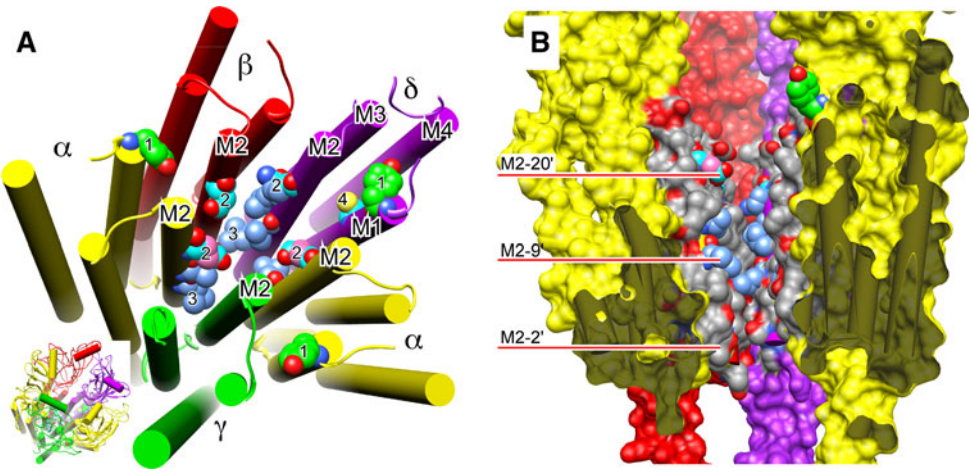

Fig. 4 Residues photolabelled on nicotinic receptors by three classes of general anesthetics. *Panel A* shows a slightly tilted top view of just the transmembrane domain of the nAChR of the nicotinic acetylcholine receptor (nAChR) from *Torpedo* using the cryoelectron microscopy structure.[20] The agonist-binding domain has been omitted for clarity, but it is shown in the inset at bottom left where the orientation is the same as in the larger diagram. The subunits are colour coded and labelled as in Fig. 2. The helices are shown as rods, and the atoms of photolabelled residues, including the backbone atoms, are shown in space-filled mode. All other residues are omitted for clarity. Oxygen (red) and nitrogen (blue) atoms are coloured conventionally. The carbon atoms are colour coded to denote which anesthetics photolabelled the residue: green, halothane; cyan, azietomidate; cornflower blue, p-Trifluoromethyldiazirinyl ethylbenzyl (TDBzl)-etomidate; salmon, azioctanol. In some cases, more than one agent photolabels the same residue, and individual carbons are given different colours accordingly. Number code: 1. αY213 and δY228 photolabelled on M1 by halothane; 2. αE262, βD268, and δQ276 (the M2-20′ residues) photolabelled by azietomidate and azioctanol; 3. αL251, δL265 (the M2-9′ residues) photolabelled by TDBzl-etomidate; 4. δC236 on M1 photolabelled by azietomidate. *Panel B* shows a cross-section through the transmembrane domain of the same nAChR structure. The γ-subunit has been removed to facilitate a view of the ion pore. The viewer is situated at the γ-subunit, and the two α-subunits are closest to the viewer. The subunits have the same colour code as before but are depicted as surfaces. The dark grey regions denote where the surface of the α-subunits have been cut through and serve to emphasize the free space that exists within the four-helix bundle of subunits. The central ion channel is open to view. The M2 helices are coloured conventionally with grey for carbon, red for oxygen, and blue for nitrogen, except that some of the carbons in photolabelled residues have the same colour code as in panel A. The red bars point to residues on M2 using the prime numbering system, where 1′ is the residue following the last charged residue before the M2 helix, and M2-9′ is always the conserved leucine

M2–20′, but it also photolabels the equivalent M2–20′ residues (βD268 and δQ276) (the γ-subunit was not examined), confirming that the upper end of the channel lies within an anesthetic binding site. On the β- and δ- subunits, there are reactive residues at M2–24′ one helical turn above their respective photolabelled M2–20′ residues. These residues, βE272 and δE280, define the limits of the binding site because they are not photolabelled, suggesting that the site extends in an intracellular direction. This hypothesis is confirmed by a second etomidate derivative bearing an aromatic diazirine in place of the aliphatic diazirine. p-Trifluoromethyldiazirinyl ethylbenzyl (TDBzl)-etomidate was designed to react with the hydrophobic residues more intracellular to the M2–20′ site photolabelled by azietomidate and azioctanol. Indeed, it photolabelled the channel lumen-facing residues in the α- and δ-subunits on M2 as far below M2–20′ as M2–9′, a distance along the channel of some 16.5 Å.

A number of other sites on the nAChR have been photolabelled by these agents, illustrating that a large receptor can have multiple anesthetic binding sites, although not all produce functional effects. The first of these sites is the agonist-binding pocket on the α-subunit, nearly 50 Å from the transmembrane domain.[36-38] It is photolabelled in the absence but not in the presence of agonist. This competitive behaviour is consistent with the observation that anesthetics decrease [^{3}H]acetylcholine binding at very high concentrations,[39] even though they enhance [^{3}H]acetylcholine binding at low concentrations by stabilizing the desensitized over the resting state.

Three further regions have been consistently photolabelled, usually at much lower levels of photoincorporation than the residues in the transmembrane domain, but no function has been ascribed to them and they are not discussed in detail here. The first is just before the intracellular end of M4[40] and close to the intracellular fenestrations described by Unwin.[20] The second region is in the lipid-protein interface. This is commonly considered to be nonspecific photolabelling because of the high concentration of photolabel that must be present in the lipid bilayer. The third region is the hint of a subunit interface site between αM2-10′ and the γ-subunit.[41]

Location of general anesthetic sites on $GABA_ARs$

The specific activity of $GABA_ARs$ in the brain is some 10,000-fold lower than that of nAChR in Torpedo electric tissue.[25] To improve the chances of success, it was necessary to develop a highly selective and potent general anesthetic photolabel. Steroids, propofol, and etomidate fall into this category. While photolabels are being developed for all three, etomidate was an attractive initial candidate because it is less hydrophobic than steroids while possessing stereoselectivity and a structure amenable to chemical modification at multiple positions (Fig. 3). The synthesis of azietomidate proved the value of this strategy. In spite of the aliphatic diazirine group, azietomidate retains the pharmacological properties of etomidate. Both are equipotent as general anesthetics and as modulators of the $GABA_AR$, at which they enhance GABA-induced currents and activate the channels in the absence of agonist.[34] The R-enantiomer of both is more potent than the S-enantiomer (the clinical drug is R-etomidate). Furthermore, in knock-in mice rendered less sensitive to etomidate by a β3–N265M point mutation in their $GABA_ARs$, both R-etomidate and R-azietomidate are about tenfold less potent than in wild-type mice.[42]

In a heterogeneous mixture of $GABA_ARs$ purified from cow brain, R-azietomidate was found to photolabel two residues in a GABA-sensitive allosteric manner.[25] The first residue was situated within the βM3 transmembrane helix at βMet-286 (the exact β-subtype could not be determined). This region was a known anesthetic determinant.[43-45] The second residue was novel. There was no hint of its importance from any previous site-directed mutagenesis studies. Azietomidate photolabelled α1M236 (and/or the homologous methionines in α2, 3, and 5), which is located on the αM1 transmembrane helix, three residues after the conserved proline. The ability to find a novel site illustrates the power of photolabelling; it provides binding site information at the level of the primary structure, independent of any preconceived hypothesis.

Using the homology model discussed earlier in this review,[25] the two methionine residues (αM236 and βM286) on separate subunits photolabelled by azietomidate are predicted to face each other across the interface between the α- and β-subunits in the transmembrane domain. Support for this arrangement comes from subsequent cysteine cross-linking studies.[29] Thus, the etomidate site is not within a single subunit's intrahelical bundle but, instead, is in the interface between two subunits (Fig. 5). The αM1 M236 is predicted to be more intracellular than βM3 M286, and their α-carbons are separated by 13 Å. This suggests that the etomidate site is between them, consistent with the lack of photolabelling at βM3 M283, which is located one helical turn more extracellular to the photolabelled M286. Reading clockwise, the arrangement of the subunits in $\alpha1\beta3\gamma2L$ $GABA_ARs$ is $\alpha1\beta3\alpha1\beta3\gamma2L$, so there are two α-β interfaces and, consequently, two etomidate binding sites. This is consistent with the prediction of the allosteric model discussed below.[15]

Thus, azietomidate photolabelling has provided the first evidence that placed an anesthetic binding site in a subunit

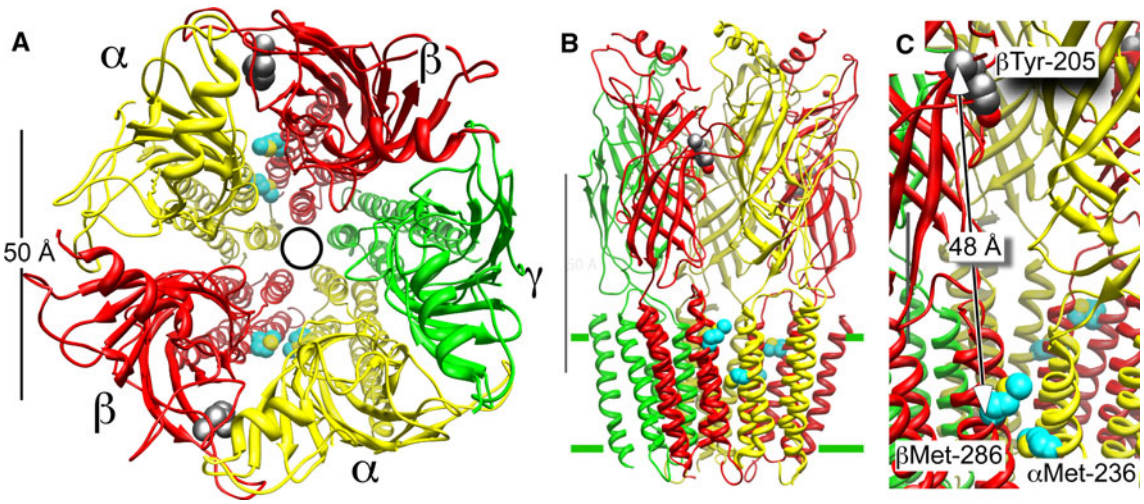

Fig. 5 Azietomidate photolabels the γ-aminobutyric acid type A receptors ($GABA_AR$) in the transmembrane domain between the α- and β-subunits. *Panel A* shows a top view from the extracellular side of the $\alpha1\beta2\gamma2L$ $GABA_AR$ homology model of Li *et al.*[25] The five subunits that are consistently colour coded in all panels are arranged centro-symmetrically around the pore, denoted by a circle. *Panel B* shows the same receptor in side view; the M3–M4 intracellular loop is omitted in this model. The scale bar is 50 Å in both panels. *Panel C* shows a detail of Panel B. The partly obscured scale bar is 20 Å. Only the secondary structure is shown except for two sets of residues. The residues with carbons shown in cyan are those photolabelled by azietomidate, αMet-236, and βMet-286, and that with dark grey carbons is βTyr-205, which is a residue in the GABA-binding pocket nearly 50 Å away

interface on a ligand-gated ion channel. While a novel concept for anesthetic mechanisms, agonist sites have long been thought to lie partly in such interfaces.[46] The agonist site in the extracellular domain, like the etomidate site in the transmembrane domain, lies in the α-β interface. The two sites are separated by $\sim$50 Å (Fig. 5C). If the agonist induces gating by perturbing the α-β interface in the transmembrane domain, it is evident that an etomidate binding site in the same interface and adjacent to the ion pore might allosterically modulate agonist gating. We return to this theme in a later section of this review. Other classes of general anesthetic have variable effects on photoincorporation of [^{3}H]azietomidate into $GABA_AR$s. These agents may have different binding sites[47]; thus, further photolabelling work with other anesthetic analogues is eagerly awaited.

Evidence for conformationally sensitive general anesthetic binding

How can we establish that the affinity of general anesthetic modulatory sites vary with the protein's conformational state (Fig. 1)? General anesthetics have such low affinities that, with rare exceptions,[14,48] nonspecific binding prevents binding to receptors from being detected. Furthermore, kinetic measurements suggest the highest affinity is often for the open state of a receptor, a transient state that is present for far too short a time to accomplish a binding measurement. Faced with this issue, time-resolved photolabelling has been adopted as a strategy for seeking sites on transient states of receptors.[49] To date, this demanding strategy has been applied only to the abundant *Torpedo* nAChR. When rapidly exposed to an agonist, the resting state of this nAChR is converted to the open state in less than a millisecond.[50,51] The entire population of open receptors is converted to the fast desensitized state a second later and to the slow desensitized state within minutes. Thus, by using time-resolved photolabelling in the absence of agonist, or 1-50 msec, one second, and minutes after rapid mixing with agonist, it is possible to determine the level of photoincorporation of an anesthetic as a function of the receptor's conformation (resting, open, fast desensitized, and slow desensitized states, respectively).[52]

The time-dependence of photoincorporation into three different anesthetic sites on the nAChR has been characterized to date (Fig. 6). All three exhibit different behaviours. The best characterized of the general

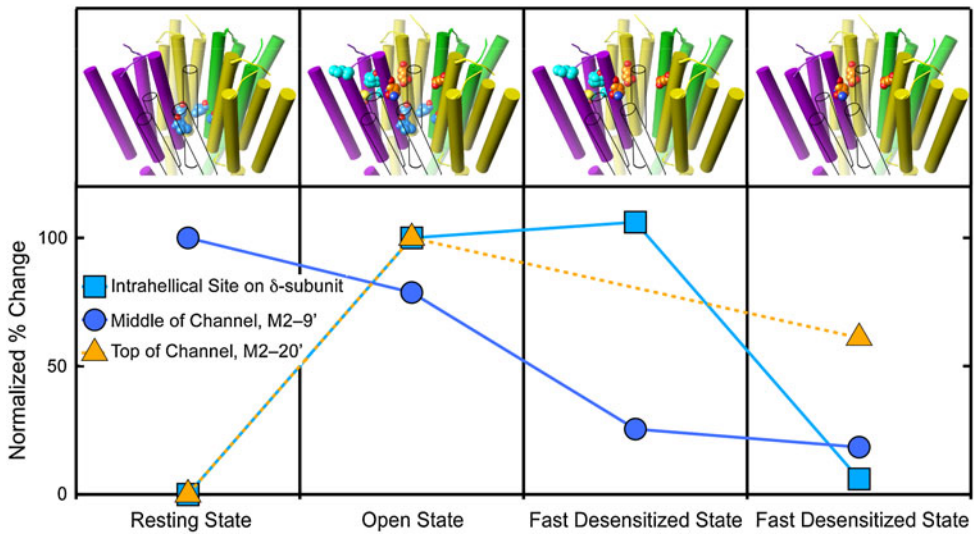

Fig. 6 The degree of photolabelling of three sites on the nicotinic acetylcholine receptor (nAChR) varies with the receptor's conformation, supporting allosteric action. The graph shows the relative level of photoincorporation for three different sites on the nicotinic acetylcholine receptor. The photoincorporation level is normalized to that first observed (either the resting or the open state). The upper panel depicts the transmembrane domain of the nAChR and the photolabelled residues in each state. The subunit colours are yellow for α, green for γ, and purple for δ. The β-subunit is shown in outline to allow only the channel residues to be seen. The carbon atoms are coloured with the same colour as the symbols on the graph. At two sites, photolabelling is negligible in the resting state but increases dramatically when the channel opens. One of these sites (orange triangles) is in the upper part of the channel (M2–20′), and the other (cyan squares) is in the intrahelical bundle of the δ-subunit. The behaviour of these sites diverges during desensitization. The channel site changes modestly, whereas the intrahelical site remains unchanged during fast desensitization and then decreases dramatically upon slow desensitization. The third site (blue circles) is also in the channel but at the conserved M2–9′ leucines. It behaves differently from the site in the upper part of the channel. It is photolabelled in the resting state and in the open state, but photolabelling decreases dramatically during fast desensitization and remains unchanged during slow desensitization. Data for azietomidate (triangles) is from[40] and for trifluoromethyl)-3-(m-iodophenyl) diazirine (TID) (circles and squares) is from[52,53]

anesthetics is azietomidate,[40] which photolabels the M2–20′ residues. These channel-lumen residues are not photolabelled in the resting state, but as soon as the channel opens, photoincorporation into these residues is robust (Fig. 6, triangles). No data are available for the fast-desensitized state, but photoincorporation falls during slow desensitization. The most complete set of data is for the hydrophobic aromatic diazirine, ^{125}I-TID (3-(trifluoromethyl)-3-(m-iodophenyl) diazirine (Fig. 3).[52,53] It photolabels the nAChR in the resting state in the centre of the channel at M2–9′, the second of the three sites. During channel opening, photoincorporation at M2–9′ falls, but by surprisingly little. It is not until the receptor enters the fast desensitized state that photoincorporation into the channel declines dramatically (Fig. 6, circles).

The third site is the transmembrane domain intrahelical site in the four-helix bundle on the δ-subunit. It is photolabelled by halothane and by azietomidate, but the best time-resolved photolabelling is with TID. This site is not photolabelled in the resting state, but it is photolabelled within 1 msec of adding acetylcholine (Fig. 6, squares). Furthermore, photoincorporation remains unchanged when the nAChR enters the fast-desensitized state, but it falls dramatically upon slow desensitization. It is interesting to note that halothane photolabels this site in the resting state, suggesting that this much smaller molecule can fit into the pocket in a conformation that cannot accommodate the larger probes, azietomidate and TID.

Do current concepts of gating and desensitization help us understand why photoincorporation into each of the three sites above has a different dependence on the nAChR conformation (Fig. 6)? The two-gate hypothesis of Auerbach and Akk[54] that postulates distinct activation and desensitization gating structures in the nAChR channel[54] offers an explanation as to why sites at two different levels within the channel lumen, i.e., at M2–9′ and at M2–20′, behave differently as the channel's conformation changes (Fig. 6). The hypothesis states that the desensitization gate is open in the resting state and the activation gate is closed. Agonist opens the activation gate and conduction occurs. During fast desensitization, the desensitization gate closes while the activation gate remains open. Thus, the structural changes associated with the activation gate correlate with photoincorporation at M2–20′ residues, whereas those associated with the desensitization gate correlate with photoincorporation at M2–9′. It is as though the channel's long sausage-shaped cavity is squeezed at different points during the conformation changes associated with opening and fast desensitization (and presumably during slow desensitization when both gates might be closed, although the model did not address this issue).

The uncoupled model of desensitization postulates that each subunit has only one desensitized structure, and that the difference between fast and slow desensitized states is in the number of subunits in their desensitized conformation.[55] Fast desensitization is associated with the γ-α subunit pair desensitizing, whereas slow desensitization is associated with the δ-α subunit pair. The M2–9′ site will be affected by the motion in any subunit, so that desensitization of the γ-α subunit pair and then the δ-α subunit pair would be sufficient to lower photoincorporation during both fast and slow desensitization, as is observed (Fig. 6). The uncoupled model is also consistent with the behaviour of the anesthetic site in the intrahelical bundle of the δ-subunit, because it remains unchanged during fast desensitization and only changes during slow desensitization. The structural basis for the δ-subunit being the only one to exhibit intrahelical binding may be that the δ-subunit is the only one that has a proline near the middle of M4. This causes the upper part of the helix to bend out into the lipid-protein interface, creating more space within the intrasubunit four-helix bundle.

Thus, a structural basis is beginning to emerge for the way in which general anesthetics interact with their binding sites as ligand-gated ion channels pass through their various functional states. That the allosteric principle applies means that it is now possible to conceive of designing agents that are selective not only for a given receptor but also for a given conformation of that receptor. Such specific design requires more detailed structural insights than are currently available, but these are likely to come. Meanwhile, functional studies are also often consistent with allosteric action. The combination of functional and structural studies will be necessary to obtain a complete description of general anesthetic action.

Allosteric co-agonism: A formal mechanism for general anesthetic actions in $GABA_A$ receptors

Formal allosteric paradigms for general anesthetic modulation of $GABA_A$ receptors rarely have been applied in molecular studies. The best-established paradigm is that for etomidate effects at $\alpha1\beta2\gamma2$L $GABA_A$ receptors,[15] essentially a two-state Monod-Wyman-Changeux (MWC) allosteric co-agonist model (Fig. 7). The underlying assumptions of MWC allosteric models, as outlined in 1965, include the existence of interchangeable conformations, both in the presence and absence of ligands, and maintenance of symmetry during structural transitions.[8] The simplest equilibrium MWC models have two interchangeable states, i.e., resting and active. Agonists in this formalism are any ligands (orthosteric or allosteric) that bind with higher affinity to active states than to inactive states. Thus, addition of agonist preferentially stabilizes open-channel conductive (active) states of ion channels.

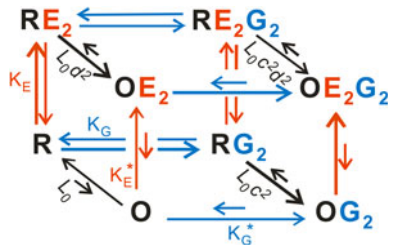

Fig. 7 The scheme depicts equilibrium two-state allosteric co-agonism for GABA and etomidate actions on γ-aminobutyric acid type A ($GABA_A$) receptors, as described by Rüsch *et al*.[15] There are two equivalent GABA sites and two equivalent etomidate sites. Only doubly-bound states are shown, both for simplicity and because they are the most highly populated states when ligands are present. GABA binding transitions are blue, etomidate binding transitions are red, and gating (opening and closing) transitions are black. The L_0 parameter describes the basal equilibrium between closed (R) and open (O) states. K_G is the dissociation constant for GABA interactions with R-state receptors and K_G* is the dissociation constant for GABA interactions with O-state receptors. The GABA efficacy factor, c, is defined as K_G*/K_G. K_E is the dissociation constant for etomidate interactions with R-state receptors, and K_E* is the dissociation constant for etomidate interactions with O-state receptors. The anesthetic efficacy factor, d, is defined as K_E*/K_E

The concept of inverse agonism is also implicit in these mechanisms; inverse agonists are agonist site ligands that bind better to inactive rather than to active states and act as competitive antagonists in the presence of full agonists.

The co-agonist model for GABA and etomidate emerged, in part, from research on $GABA_A$ receptor mutations and other anesthetics. A similar model has been considered previously for barbiturate actions on $GABA_A$ receptors.[56] In 1999, Chang and Weiss demonstrated that a two-state equilibrium MWC allosteric model describes GABA-dependent activation of $GABA_A$ receptors harbouring mutations at the highly conserved M2–9′ leucines.[57] When L9′ residues are mutated to serines or threonines, enhancement is produced of *both* basal receptor-channel gating activity and apparent GABA sensitivity, effects that are similar to those observed in the presence of general anesthetics. In addition, studies showed that potentiation of $GABA_A$ receptor responses to partial agonists by propofol[58] and barbiturates[59] is due to increased agonist efficacy rather than to enhanced agonist binding at the orthosteric (GABA) binding site.

For etomidate, other critical observations supported a MWC co-agonist mechanism. First, etomidate displays significant stereospecific actions as an anesthetic, paralleling its stereospecificity at $GABA_A$ receptors and providing convincing evidence for a protein site or sites of action.[34,60,61] Like a number of other general anesthetics, etomidate potentiates GABA-dependent receptor activation, resulting in enhanced apparent GABA sensitivity. Furthermore, high concentrations of etomidate directly activate $GABA_A$ receptors in the absence of orthosteric agonists, an action termed direct activation or GABA-mimetic activity.[61-63] Notably, the tenfold to twentyfold R(+)/S(-) stereoselectivity observed for GABA potentiation of $GABA_A$ receptors was the same magnitude as that seen for direct activation by etomidate.[34,60] In addition, subunit substitutions and mutations that reduced $GABA_A$ receptor sensitivity to GABA potentiation also reduced direct activation by etomidate.[63,64] These observations suggest that a single class of allosteric etomidate sites may underlie both potentiation of GABA responses and direct receptor activation.

An alternative hypothesis is that the GABA-potentiating and direct activating effects of general anesthetics are mediated respectively by distinct high- and low-affinity sites on $GABA_A$ receptors.[65] Support for the existence of high-affinity anesthetic sites depends on the methods used to quantify GABA potentiation. In particular, the presence of high-affinity sites has been inferred frequently from measurements of anesthetic potentiation at a single GABA concentration, usually EC5 or EC10. The flaw in this approach is that the half-effect anesthetic enhancing concentration varies depending on the amount of GABA activation being enhanced. Thus, if one assumes that saturating GABA activates nearly all receptors (i.e., intrinsic efficacy is about 1.0), then an anesthetic concentration that enhances activation tenfold will produce a maximum effect in the presence of GABA at EC10. In other words, the observable amount of enhancement has a "ceiling" around tenfold. Under these conditions, the half-effect anesthetic concentration will produce a 4.5-fold enhancement (halfway between onefold and tenfold). However, in a similar experiment performed using GABA at EC25, the anesthetic concentration that quadruples activation will produce maximal activation, and the half-effect anesthetic concentration will enhance activation by only 1.5-fold. In contrast, assessing allosteric enhancement from shifts in agonist response curves eliminates the "ceiling effect." When etomidate-induced GABA potentiation was assessed using leftward shifts of concentration-responses curves, no evidence for high-affinity sites was found,[15] suggesting that both direct activation and agonist enhancement might be mediated by a single class of low-affinity sites by anesthetic binding.

The MWC co-agonist model (Fig. 7) explains anesthetic actions by postulating a single class of allosteric anesthetic sites that act as co-agonist sites linked to the receptor gating equilibrium. Monod-Wyman-Changeux analysis of wild-type $\alpha1\beta2\gamma2L$ $GABA_A$ receptor function quantitatively accounts for direct activation, enhancement of currents elicited with GABA EC5, and etomidate-dependent shifts in GABA effective concentration $(EC)_{50}$. It also quantitatively accounts for effects of combining etomidate with a partial agonist.[15] Moreover, models postulating two

equivalent etomidate sites fit the data significantly better than models assuming different numbers of etomidate sites, a conclusion that accurately predicted subsequent azietomidate photolabelling results.[25]

Allosteric co-agonism as a framework for structure-function analysis

The MWC allosteric co-agonist model has proven to be a powerful tool for analysis of structure-function studies of etomidate interactions with $GABA_A$ receptors. An idea that emerges directly from MWC allosteric principles is that receptors (including certain wild-type $GABA_A$ subunit combinations, and also mutants) can activate spontaneously in the absence of agonists. Furthermore, as Chang and Weiss observed, more spontaneous activity is associated with an apparent higher affinity for agonists. Thus, the co-agonist mechanism correctly predicts that spontaneously active $GABA_A$ receptors with an L9′S or L9′T gating mutation are exquisitely sensitive to direct activation by etomidate.[15] Indeed, assessment of spontaneous activity in $GABA_A$ receptor mutants is a critical factor in MWC allosteric models. Wild-type $\alpha1\beta2\gamma2L$ receptors are estimated to have a very low spontaneous activity ($P_0 < 0.0001$), and experimentally, it is difficult to measure activity this low. However, when the impact of a mutation on spontaneous activity is small, it can be estimated using mutant-cycle analysis by adding a second mutant subunit containing an L9′S or L9′T.[66]

To date, the MWC co-agonist framework has been used to analyze the effects of $GABA_A$ receptor mutations at three amino acids that are hypothesized to interact with etomidate.[66,67] Two of these residues, αM236 and βM286, were identified by azietomidate photolabelling of purified detergent-solubilized bovine brain receptors[25] (see *Location of general anesthetic sites on $GABA_A$ receptors*, above). Stewart *et al.*[67] hypothesized that bulky hydrophobic tryptophan side chains at these residues would occupy the space where etomidate binds. The β2M286W mutation in the $\alpha1\beta2\gamma2$ background increases receptor sensitivity to GABA and produces spontaneous gating in the absence of GABA, which is detectable using picrotoxin (Table 1). These functional characteristics of the mutant channel mimic the impact of etomidate binding.[67] In addition, in the presence of etomidate, β2M286W channels display neither GABA modulation nor direct activation. In the absence of etomidate-dependent effects, model fitting to these data fails to indicate whether etomidate binding or efficacy is reduced by the mutation (Table 2). Similar to β2M286W, the α1M236W mutation produces receptors with increased GABA sensitivity relative to wild-type and spontaneous activation, mimicking the effects of etomidate binding to wild-type receptors. Notably, receptors harbouring α1M236W mutations are potently and efficaciously activated by etomidate, while modulation of GABA responses by etomidate is much weaker than that observed in wild-type receptors. Monod-Wyman-Changeux modelling proves valuable in making sense of this pattern of results. The small leftward shift of GABA responses results in a low etomidate efficacy factor in the fitted model, but this low efficacy is sufficient to activate fully those channels that have a strong propensity to open based on their spontaneous activity.

Another $GABA_A$ receptor residue of great interest is β2N265 (M2–15′), which faces away from the transmembrane pore in homology models. Mutations at this site on the pore-forming M2 helix were first reported to reduce etomidate and loreclezole sensitivity dramatically.[63] Furthermore, mice with knock-in mutations β2N265S or β3N265M have normal baseline phenotypes but markedly altered behavioural sensitivity to various etomidate, propofol, and barbiturate actions.[1,68] Compared with wild-type receptors in oocytes, $\alpha1\beta2N265S\gamma2L$ receptors display no

Table 1 Functional characteristics of wild-type and mutant $GABA_A$ receptors activated with GABA ± etomidate

Receptor	Spontaneous Activation*	GABA EC_{50} (μM)	GABA Efficacy†	Etomidate EC_{50} (μM)	Etomidate Efficacy‡	Left-Shift Ratio (CNTL/ETO)
$\alpha1\beta2\gamma2L$	<0.001	26	0.9	36	0.4	20
$\alpha1M236W\beta2\gamma2L$	0.16	2.0	0.99	12	0.97	1.7
$\alpha1\beta2M286W\gamma2L$	0.04	6.6	1.0	NA	<0.001	1.1
$\alpha1\beta2N265S\gamma2L$	<0.001	27	0.93	78	0.03	2.3
$\alpha1\beta2N265M\gamma2L$	<0.001	32	0.84	NA	<0.001	0.95

* Spontaneous activation is estimated using picrotoxin to block constitutively active receptors in the absence of agonists. The picrotoxin-sensitive current was normalized to the maximum GABA current.

† GABA efficacy is estimated using positive allosteric modulators (etomidate or alphaxalone) to enhance the maximum current elicited by high GABA concentrations. We assume that the combination of high GABA plus allosteric enhancer activates all receptors.

‡ Etomidate efficacy is the maximum current elicited by etomidate, normalized to the maximum current elicited with GABA. $GABA_A$ = γ-aminobutyric acid type A receptors; EC_{50} = effective concentration; CNTL = control measured in the absence of etomidate; ETO = etomidate.

Table 2 Monod-Wyman-Changeux co-agonist model parameters for wild-type and mutant $GABA_A$ receptors activated with GABA ± etomidate

Receptor	L_0	K_G (μM)	c	K_E (μM)	d
$\alpha1\beta2\gamma2L$	25,000	70	0.0019	40	0.0077
$\alpha1M236W\beta2\gamma2L$	6.2	51	0.021	24	0.18
$\alpha1\beta2M286W\gamma2L$	31	32	0.029	NA	NA
$\alpha1\beta2N265S\gamma2L$	25,000	68	0.0018	88	0.038
$\alpha1\beta2N265M\gamma2L$	50,000	59	0.0019	NA	NA

The allosteric model parameters are described in the legend to Fig. 1. L_0 was estimated as described in Desai *et al.*[66] Parameters were fit by non-linear least squares as described in Desai *et al.*[66] $GABA_A$ = γ-aminobutyric acid type A receptors; c = GABA efficacy factor; d = anesthetic efficacy factor; NA = not available.

change in basal gating, GABA EC_{50}, or GABA efficacy.[66] The β2N265M mutation slightly increases GABA EC_{50} and reduces GABA efficacy. Combining this mutation with the α1L264T mutation that produces spontaneous activation reveals that the β2N265M mutation reduces spontaneous gating about twofold, which accounts for both its altered GABA EC_{50} and its efficacy. Both α1N265 mutations also confer etomidate insensitivity. The β2N265S mutation reduces both GABA modulation and direct activation by etomidate, while β2N265M eliminates these etomidate effects. The MWC co-agonist model fitting to the data set for β2N265S suggests that etomidate efficacy is reduced far more than etomidate affinity to resting receptors. Nonetheless, efficacy in the context of MWC models represents the relative affinity for active *vs* inactive receptors. Thus, βN265 mutations appear to have no effect on etomidate binding to resting (closed) receptors, but βN265 may contact etomidate in open receptors, where M and S mutations weaken binding.

The framework of MWC allosteric co-agonism has also proven valuable in designing protection studies based on cysteine substitutions and modification with small sulfhydryl-modifying probes. Prior work, notably in the labs of Akabas[43,69] and Czajkowski,[70] have shown that the rate of sulfhydryl modification is often dependent on whether receptors are closed *vs* active. Therefore, to interpret protection studies properly when it is hypothesized that ligands sterically interfere with sulfhydryl modification, one must identify control and protection conditions where the distribution of resting *vs* activated receptors is similar. Furthermore, protection can best be demonstrated when ligand occupancy is high and when that ligand has agonist activity. As with anesthetics at $GABA_A$ receptors, the problem is complicated further by the protective ligand altering the distribution of resting and activated receptors. The approach used in our lab to provide a framework for designing optimal protection experiments has been to "phenotype" cysteine substituted mutant receptors using the MWC co-agonist model, including measurement of spontaneous activation, GABA binding and efficacy, and anesthetic binding and efficacy. The results (not yet published) provide a more solid basis for inferences about which $GABA_A$ receptor residues interact with general anesthetics.

Can allosteric co-agonism at $GABA_A$ receptors be generalized to other drugs and experiments?

So far, simple equilibrium MWC co-agonist models appear to work well for the analysis of oocyte electrophysiology data for $GABA_A$ receptors, where the relatively slow rate of drug concentration changes may result in mixing of receptors in activated and desensitized states. Further experiments will be required to determine if similar or related models will be useful for interpreting rapid kinetic patch-clamp electrophysiological data, single-channel kinetic data, or other types of dynamic signals, such as those from fluorescent labels within $GABA_A$ receptors. The concept of allosteric agonism will likely be a useful framework for interpreting the actions of other general anesthetic drugs. Structural studies locating the high-affinity benzodiazepine binding site at a position homologous to the orthosteric agonist (GABA) binding sites suggested that these drugs might be allosteric agonists. This premise was shown to be the case in two ways. First, benzodiazepine agonists were shown to gate spontaneously active mutant $\alpha1L264T\beta2\gamma2L$ $GABA_A$ receptors directly, approximately tripling open probability. Thus, benzodiazepine agonists directly enhance the gating of these receptors in the absence of orthosteric agonists. Second, when wild-type $\alpha1\beta2\gamma2L$ $GABA_A$ receptors are maximally activated with the partial agonist, P4S, addition of benzodiazepine agonists increases the maximal current, indicating that these drugs also increase gating efficacy under conditions where orthosteric sites are fully occupied by agonist.[71]

There is related data supporting the idea that propofol and barbiturates, and perhaps neurosteroids, act as allosteric agonists at $GABA_A$ receptors. We have noted already that propofol and barbiturates enhance the efficacy of partial agonists, indicating that they affect gating rather than agonist binding. At supra-clinical concentrations, barbiturates, propofol, and volatiles also directly activate synaptic $GABA_A$ receptors. The single-channel conductance elicited with barbiturates matches that elicited using GABA, supporting the assumption that similar, if not identical, conformational changes are triggered by these two classes of agonist.[59,72] Similarly, cysteine accessibility and cross-linking studies in the channel-lining M2 helices of $GABA_A$ receptors indicate that channel structure is similar when opened by both GABA and propofol.[73]

Can propofol actions at $GABA_A$ receptors be described by an allosteric co-agonist mechanism similar to that for etomidate? We have addressed this question by comparing the linkages between direct activation and GABA modulation for both propofol and etomidate. Using oocyte electrophysiology, we identified a propofol concentration that is equipotent with 10 μM etomidate for direct activation of $\alpha1\beta2\gamma2$L $GABA_A$ receptors. Preliminary studies demonstrate that the shift in GABA concentration-responses produced by this propofol concentration matches that produced by 10 μM etomidate. Thus, the linkage between direct agonism and GABA modulation inherent in co-agonist models is maintained for propofol. Additional experiments are underway to establish the number of equivalent propofol sites that best fits the MWC model.

Emerging hypotheses regarding anesthetic modulation sites on Cys-loop ion channels

Research during the previous two decades has tremendously improved our understanding of the mechanisms underlying general anesthetics. In the case of etomidate, transgenic animal studies[1,68] have confirmed that the major molecular targets are $GABA_A$ receptors. The major functional effects of drug binding to targets are explained by allosteric co-agonism,[15] and photolabelling has identified the binding sites amidst transmembrane helices.[25] Additional potential binding sites of this type exist both within the four TM helices of single Cys-loop ion channel subunits and also within the transmembrane pore and at subunit interfaces. Indeed, recent data suggest that the sites where neurosteroids and propofol bind to $GABA_A$ receptors differ from those for etomidate.[47] The formal functional paradigm presented for etomidate may apply to these other potent general anesthetic drugs. Combining photolabelling with structure-function mutational studies in the context of allosteric mechanisms should lead us to a more detailed understanding of how and where these important drugs act.

Funding sources Funded by a grant from the National Institute of General Medical Sciences (GM 58448) and by the Department of Anesthesia, Critical Care and Pain Medicine, Massachusetts General Hospital.

Conflicts of interest None declared.

References

1. *Jurd R*, *Arras M*, *Lambert S*, *et al*. General anesthetic actions in vivo strongly attenuated by a point mutation in the GABA(A) receptor beta3 subunit. FASEB J 2003; 17: 250-2.
2. *Campagna JA*, *Miller KW*, *Forman SA*. Mechanisms of actions of inhaled anesthetics. N Engl J Med 2003; 348: 2110-24.
3. *Hemmings HC Jr*, *Akabas MH*, *Goldstein PA*, *Trudell JR*, *Orser BA*, *Harrison NL*. Emerging molecular mechanisms of general anesthetic action. Trends Pharmacol Sci 2005; 26: 503-10.
4. *Rudolph U*, *Antkowiak B*. Molecular and neuronal substrates for general anaesthetics. Nat Rev Neurosci 2004; 5: 709-20.
5. *Grasshoff C*, *Drexler B*, *Rudolph U*, *Antkowiak B*. Anaesthetic drugs: linking molecular actions to clinical effects. Curr Pharm Des 2006; 12: 3665-79.
6. *Zeller A, Jurd R, Lambert S, et al.* Inhibitory ligand-gated ion channels as substrates for general anesthetic actions. Handb Exp Pharmacol 2008; 31-51.
7. *Franks NP*. General anaesthesia: from molecular targets to neuronal pathways of sleep and arousal. Nat Rev Neurosci 2008; 9: 370-86.
8. *Monod J*, *Wyman J*, *Changeux JP*. On the nature of allosteric transitions: a plausible model. J Mol Biol 1965; 12: 88-118.
9. *Perutz MF*. Mechanisms of cooperativity and allosteric regulation in proteins. Q Rev Biophys 1989; 22: 139-237.
10. *Cui Q*, *Karplus M*. Allostery and cooperativity revisited. Protein Sci 2008; 17: 1295-307.
11. *Changeux JP*, *Taly A*. Nicotinic receptors, allosteric proteins and medicine. Trends Mol Med 2008; 14: 93-102.
12. *Taly A*, *Corringer PJ*, *Guedin D*, *Lestage P*, *Changeux JP*. Nicotinic receptors: allosteric transitions and therapeutic targets in the nervous system. Nat Rev Drug Discov 2009; 8: 733-50.
13. *Changeux JP*, *Edelstein SJ*. Allosteric mechanisms of signal transduction. Science 2005; 308: 1424-8.
14. *Dodson BA*, *Braswell LM*, *Miller KW*. Barbiturates bind to an allosteric regulatory site on nicotinic acetylcholine receptor-rich membranes. Mol Pharmacol 1987; 32: 119-26.
15. *Rusch D*, *Zhong H*, *Forman SA*. Gating allosterism at a single class of etomidate sites on alpha1beta2gamma2L GABA-A receptors accounts for both direct activation and agonist modulation. J Biol Chem 2004; 279: 20982-92.
16. *Arias HR*, *Kem WR*, *Trudell JR*, *Blanton MP*. Unique general anesthetic binding sites within distinct conformational states of the nicotinic acetylcholine receptor. Int Rev Neurobiol 2003; 54: 1-50.
17. *Baenziger JE, Corringer PJ.* 3D structure and allosteric modulation of the transmembrane domain of pentameric ligand-gated ion channels. Neuropharmacology 2010; DOI: 10.1016/j.neuropharm.2010.08.007.
18. *Olsen RW*, *Chang CS*, *Li G*, *Hanchar HJ*, *Wallner M*. Fishing for allosteric sites on GABA(A) receptors. Biochem Pharmacol 2004; 68: 1675-84.
19. *Miller KW*. The nature of sites of general anaesthetic action. Br J Anaesth 2002; 89: 17-31.
20. *Unwin N*. Refined structure of the nicotinic acetylcholine receptor at 4Å resolution. J Mol Biol 2005; 346: 967-89.
21. *Bocquet N*, *Nury H*, *Baaden M*, *et al*. X-ray structure of a pentameric ligand-gated ion channel in an apparently open conformation. Nature 2009; 457: 111-4.
22. *Hilf RJ*, *Dutzler R*. Structure of a potentially open state of a proton-activated pentameric ligand-gated ion channel. Nature 2009; 457: 115-8.
23. *Weng Y*, *Yang L*, *Corringer PJ*, *Sonner JM*. Anesthetic sensitivity of the Gloeobacter violaceus proton-gated ion channel. Anesth Analg 2010; 110: 59-63.
24. *Nury H, Van Renterghem C, Weng Y, et al.* X-ray structures of general anaesthetics bound to a pentameric ligand-gated ion channel. Nature 2010; in press.
25. *Li GD*, *Chiara DC*, *Sawyer GW*, *Husain SS*, *Olsen RW*, *Cohen JB*. Identification of a $GABA_A$ receptor anesthetic binding site at subunit interfaces by photolabeling with an etomidate analog. J Neurosci 2006; 26: 11599-605.

26. *Campagna-Slater V*, *Weaver DF*. Molecular modelling of the GABAA ion channel protein. J Mol Graph Model 2007; 25: 721-30.
27. *Ernst M*, *Bruckner S*, *Boresch S*, *Sieghart W*. Comparative models of GABAA receptor extracellular and transmembrane domains: important insights in pharmacology and function. Mol Pharmacol 2005; 68: 1291-300.
28. *Jansen M*, *Akabas MH*. State-dependent cross-linking of the M2 and M3 segments: functional basis for the alignment of GABAA and acetylcholine receptor M3 segments. J Neurosci 2006; 26: 4492-9.
29. *Bali M*, *Jansen M*, *Akabas MH*. GABA-induced intersubunit conformational movement in the GABAA receptor alpha 1M1-beta 2M3 transmembrane subunit interface: experimental basis for homology modeling of an intravenous anesthetic binding site. J Neurosci 2009; 29: 3083-92.
30. *Dostalova Z, Liu A, Zhou X, et al.* High-level expression and purification of Cys-loop ligand-gated ion channels in a tetracycline-inducible stable mammalian cell line: GABA(A) and serotonin receptors. Protein Sci 2010; 19: 1728–38.
31. *Bosterling B*, *Trevor A*, *Trudell JR*. Binding of halothane-free radicals to fatty acids following UV irradiation. Anesthesiology 1982; 56: 380-4.
32. *el-Maghrabi EA*, *Eckenhoff RG*, *Shuman H*. Saturable binding of halothane to rat brain synaptosomes. Proc Natl Acad Sci USA 1992; 89: 4329-32.
33. *Husain SS*, *Forman SA*, *Kloczewiak MA*, *et al*. Synthesis and properties of 3-(2-hydroxyethyl)-3-n-pentyldiazirine, a photoactivable general anesthetic. J Med Chem 1999; 42: 3300-7.
34. *Husain SS*, *Ziebell MR*, *Ruesch D*, *et al*. 2-(3-Methyl-3H-diaziren-3-yl)ethyl 1-(1-phenylethyl)-1H-imidazole-5-carboxylate: a derivative of the stereoselective general anesthetic etomidate for photolabeling ligand-gated ion channels. J Med Chem 2003; 46: 1257-65.
35. *Eckenhoff RG*, *Xi J*, *Shimaoka M*, *Bhattacharji A*, *Covarrubias M*, *Dailey WP*. Azi-isoflurane, a photolabel analog of the commonly used inhaled general anesthetic isoflurane. ACS Chem Neurosci 2010; 1: 139-45.
36. *Pratt MB*, *Husain SS*, *Miller KW*, *Cohen JB*. Identification of sites of incorporation in the nicotinic acetylcholine receptor of a photoactivatible general anesthetic. J Biol Chem 2000; 275: 29441-51.
37. *Chiara DC*, *Dangott LJ*, *Eckenhoff RG*, *Cohen JB*. Identification of nicotinic acetylcholine receptor amino acids photolabeled by the volatile anesthetic halothane. Biochemistry 2003; 42: 13457-67.
38. *Ziebell MR*, *Nirthanan S*, *Husain SS*, *Miller KW*, *Cohen JB*. Identification of binding sites in the nicotinic acetylcholine receptor for [^{3}H]azietomidate, a photoactivatable general anesthetic. J Biol Chem 2004; 279: 17640-9.
39. *Firestone LL*, *Sauter JF*, *Braswell LM*, *Miller KW*. Actions of general anesthetics on acetylcholine receptor-rich membranes from Torpedo californica. Anesthesiology 1986; 64: 694-702.
40. *Chiara DC*, *Hong FH*, *Arevalo E*, *et al*. Time-resolved photolabeling of the nicotinic acetylcholine receptor by [3H]azietomidate, an open-state inhibitor. Mol Pharmacol 2009; 75: 1084-95.
41. *Nirthanan S*, *Garcia G 3rd*, *Chiara DC*, *Husain SS*, *Cohen JB*. Identification of binding sites in the nicotinic acetylcholine receptor for TDBzl-etomidate, a photoreactive positive allosteric effector. J Biol Chem 2008; 283: 22051-62.
42. *Liao M*, *Sonner JM*, *Husain SS*, *et al*. R (+) etomidate and the photoactivable R (+) azietomidate have comparable anesthetic activity in wild-type mice and comparably decreased activity in mice with a N265M point mutation in the gamma-aminobutyric acid receptor beta3 subunit. Anesth Analg 2005; 101: 131-5.
43. *Bali M*, *Akabas MH*. Defining the propofol binding site location on the GABAA receptor. Mol Pharmacol 2004; 65: 68-76.
44. *Krasowski MD*, *Koltchine W*, *Rick CE*, *Ye Q*, *Finn SE*, *Harrison NL*. Propofol and other intravenous anesthetics have sites of action on the gamma-aminobutyric acid type A receptor distinct from that for isoflurane. Mol Pharmacol 1998; 53: 530-8.
45. *Mihic SJ*, *Ye Q*, *Wick MJ*, *et al*. Sites of alcohol and volatile anaesthetic action on GABA(A) and glycine receptors. Nature 1997; 389: 385-9.
46. *Grutter T*, *Changeux JP*. Nicotinic receptors in wonderland. Trends Biochem Sci 2001; 26: 459-63.
47. *Li GD*, *Chiara DC*, *Cohen JB*, *Olsen RW*. Numerous classes of general anesthetics inhibit etomidate binding to gamma-aminobutyric acid type A (GABAA) receptors. J Biol Chem 2010; 285: 8615-20.
48. *Roth SH*, *Forman SA*, *Braswell LM*, *Miller KW*. Actions of pentobarbital enantiomers on nicotinic cholinergic receptors. Mol Pharmacol 1989; 36: 874-80.
49. *Miller KW*, *Addona GH*, *Kloczewiak MA*. Approaches to proving there are general anesthetic sites on ligand gated ion channels. Toxicol Lett 1998; 100–101: 139-47.
50. *Forman SA*, *Miller KW*. High acetylcholine concentrations cause rapid inactivation before fast desensitization in nicotinic acetylcholine receptors from Torpedo. Biophys J 1988; 54: 149-58.
51. *Maconochie DJ*, *Steinbach JH*. The channel opening rate of adult- and fetal-type mouse muscle nicotinic receptors activated by acetylcholine. J Physiol 1998; 506: 53-72.
52. *Yamodo IH*, *Chiara DC*, *Cohen JB*, *Miller KW*. Conformational changes in the nicotinic acetylcholine receptor during gating and desensitization. Biochemistry 2010; 49: 156-65.
53. *Arevalo E*, *Chiara DC*, *Forman SA*, *Cohen JB*, *Miller KW*. Gating-enhanced accessibility of hydrophobic sites within the transmembrane region of the nicotinic acetylcholine receptor's {delta}-subunit. A time-resolved photolabeling study. J Biol Chem 2005; 280: 13631-40.
54. *Auerbach A*, *Akk G*. Desensitization of mouse nicotinic acetylcholine receptor channels. A two-gate mechanism. J Gen Physiol 1998; 112: 181-97.
55. *Andreeva IE, Pedersen SE.* Conformational asymmetry of nicotinic acetylcholine receptor (AChR) desensitization. Biophys J 2005; 89: 3052–Pos.
56. *Cash DJ*, *Subbarao K*. Different effects of pentobarbital on two gamma-aminobutyrate receptors from rat brain: channel opening, desensitization, and an additional conformational change. Biochemistry 1988; 27: 4580-90.
57. *Chang Y*, *Weiss DS*. Allosteric activation mechanism of the alpha1beta2gamma2 gamma-aminobutyric acid type A receptor revealed by mutation of the conserved M2 leucine. Biophys J 1999; 77: 2542-51.
58. *O'Shea SM*, *Wong LC*, *Harrison NL*. Propofol increases agonist efficacy at the GABA(A) receptor. Brain Res 2000; 852: 344-8.
59. *Steinbach JH*, *Akk G*. Modulation of GABA(A) receptor channel gating by pentobarbital. J Physiol 2001; 537: 715-33.
60. *Belelli D*, *Muntoni AL*, *Merrywest SD*, *et al*. The in vitro and in vivo enantioselectivity of etomidate implicates the $GABA_A$ receptor in general anaesthesia. Neuropharmacology 2003; 45: 57-71.
61. *Tomlin SL*, *Jenkins A*, *Lieb WR*, *Franks NP*. Stereoselective effects of etomidate optical isomers on gamma-aminobutyric acid type A receptors and animals. Anesthesiology 1998; 88: 708-17.
62. *Yang J*, *Uchida I*. Mechanisms of etomidate potentiation of GABAA receptor-gated currents in cultured postnatal hippocampal neurons. Neuroscience 1996; 73: 69-78.
63. *Belelli D*, *Lambert JJ*, *Peters JA*, *Wafford K*, *Whiting PJ*. The interaction of the general anesthetic etomidate with the gamma-

aminobutyric acid type A receptor is influenced by a single amino acid. Proc Natl Acad Sci USA 1997; 94: 11031-6.
64. *Hill-Venning C*, *Belelli D*, *Peters JA*, *Lambert JJ*. Subunit-dependent interaction of the general anaesthetic etomidate with the gamma-aminobutyric acid type A receptor. Br J Pharmacol 1997; 120: 749-56.
65. *Hosie AM*, *Wilkins ME*, *da Silva HM*, *Smart TG*. Endogenous neurosteroids regulate GABAA receptors through two discrete transmembrane sites. Nature 2006; 444: 486-9.
66. *Desai R*, *Ruesch D*, *Forman SA*. Gamma-amino butyric acid type A receptor mutations at β2N265 alter etomidate efficacy while preserving basal and agonist-dependent activity. Anesthesiology 2009; 111: 774-84.
67. *Stewart D, Desai R, Cheng Q, Liu A, Forman SA*. Tryptophan mutations at azi-etomidate photo-incorporation sites on alpha1 or beta2 subunits enhance GABAA receptor gating and reduce etomidate modulation Mol Pharmacol 2008; 74: 1687-95
68. *McKernan RM*, *Rosahl TW*, *Reynolds DS*, *et al*. Sedative but not anxiolytic properties of benzodiazepines are mediated by the GABA(A) receptor alpha1 subtype. Nat Neurosci 2000; 3: 587-92.
69. *Williams DB*, *Akabas MH*. Gamma-aminobutyric acid increases the water accessibility of M3 Membrane-spanning segment residues in gamma-aminobutyric acid type A receptors. Biophys J 1999; 77: 2563-74.
70. *Mercado J*, *Czajkowski C*. Gamma-aminobutyric acid (GABA) and pentobarbital induce different conformational rearrangements in the GABA A receptor alpha1 and beta2 pre-M1 regions. J Biol Chem 2008; 283: 15250-7.
71. *Rusch D*, *Forman SA*. Classic benzodiazepines modulate the open-close equilibrium in alpha1beta2gamma2L gamma-aminobutyric acid type A receptors. Anesthesiology 2005; 102: 783-92.
72. *Akk G*, *Steinbach JH*. Activation and block of recombinant GABA(A) receptors by pentobarbitone: a single-channel study. Br J Pharmacol 2000; 130: 249-58.
73. *Rosen A*, *Bali M*, *Horenstein J*, *Akabas MH*. Channel opening by anesthetics and GABA induces similar changes in the GABAA receptor M2 segment. Biophys J 2007; 92: 3130-9.
74. *Pettersen EF*, *Goddard TD*, *Huang CC*, *et al*. UCSF Chimera–a visualization system for exploratory research and analysis. J Comput Chem 2004; 25: 1605-12.